Graph Theoretic Modeling and Energy Analysis of Wireless Telemetry Networks

Tristan A. Shatto, Kurt L. Kosbar, and Egemen K. Çetinkaya
Telemetry Learning Center
Department of Electrical and Computer Engineering
Missouri University of Science and Technology
Rolla, MO 65409, USA
{taszrc, kosbar, cetinkayae}@mst.edu

Faculty Advisors:
Egemen K. Çetinkaya and Kurt L. Kosbar

ABSTRACT

Network science provides essential tools to model and analyze topology and structure of dynamic wireless telemetry networks. In this paper, we model wireless telemetry networks using three well-known graph models: Gilbert random graph, Erdős-Rényi random graph, and random geometric graph models. Next, we analyze the connectivity of synthetically generated topologies using graph energy, which is the sum of absolute values of eigenvalues. Our results indicate second-order curves for adjacency and Laplacian energies as the connectivity of synthetically generated networks improve. The normalized Laplacian energy decreases, converging to the theoretical lower bound as the connectivity reaches to a maximum.

I. INTRODUCTION AND MOTIVATION

Network science is instrumental in analysis, design, and prediction of many military applications [1, 2]. Understanding the network behavior and improving the performance of networks is one of the essential areas of developing a strong network science capability for future military scenarios. Some applications areas include: the Darknet analysis of terror networks [3] and planning and developing future scenarios [4]. Accurate, realistic, and predictive modeling of a variety of military scenarios is still in the forefront of the network science [1, 2].

Temporal networks (also called dynamic or time-varying networks) are types of network whose structural properties vary over time [5]. Examples include social networks in which relations between entities change over time, biological networks in which protein interactions are dynamic, and wireless networks in which nodes might not have stable connectivity with their neighboring nodes as wired networks do. With respect to the time-varying wireless telemetry military application, a wireless airborne telemetry network scenario has been modeled and simulated using a predictive routing algorithm [6].

Capturing the topological and structural properties of networks have been studied widely [7]. Recently, we have been looking into the rigorous mathematical property of networks by means of eigenvalues, which are the roots of the characteristic polynomial. We studied eigenvalue multiplicities of the normalized Laplacian as the nodes and links are removed from backbone networks intelligently and found that eigenvalues approach to 0 when networks are under targeted attacks [8]. We also studied the graph energy, which is the sum of absolute values of eigenvalues, of backbone networks and found that as nodes are removed graph energy decreases with the exception of normalized Laplacian [9, 10].

In this paper, we simulate wireless telemetry networks using the well-known Gilbert random graph [11], Erdős-Rényi random graph [12], and random geometric graph models [13]. We then analyze the connectivity of these synthetically generated topologies using adjacency energy [14], Laplacian energy [15], and normalized Laplacian energy [16] measures. Our results indicate that adjacency and Laplacian energies reach a peak value before converging to the stable energy level for the full-mesh type of graph. The normalized Laplacian energy consistently shows a decreasing value before merging to the theoretical lower bound.

The rest of the paper is organized as follows: The background, including definitions and simple example about the energy of graphs is presented in Section II. The description of random graph models used in this paper is presented in Section III. In Section IV, we analyze three types of graph energies for the random graphs for varying node numbers. We conclude and showcase future work in Section V.

II. GRAPH ENERGY

Let $G = (V, E)$ be an unweighted, undirected graph with n vertices and l edges. The vertex set is denoted by $V = \{v_0, v_1, \ldots, v_{n-1}\}$ and the edge set is denoted by $E = \{e_0, e_1, \ldots, e_{l-1}\}$ for G. The graph connectivity can be represented by several structures such as an adjacency matrix, Laplacian matrix, and normalized Laplacian matrix. $A(G)$ is the symmetric adjacency matrix with no self-loops, where $a_{ii} = 0$, $a_{ij} = a_{ji} = 1$ if there is a link between $\{v_i, v_j\}$, and $a_{ij} = a_{ji} = 0$ if there is no link between $\{v_i, v_j\}$. The Laplacian matrix of G is: $L(G) = D(G) - A(G)$ where $D(G)$ is the diagonal matrix of node degrees, $d_{ii} = \deg(v_i)$. Given the degree of a node is $d_i = d(v_i)$, the normalized Laplacian matrix $\mathcal{L}(G)$ is denoted:

$$\mathcal{L}(G)(i,j) = \begin{cases} 1, & \text{if } i = j \text{ and } d_i \neq 0 \\ -\dfrac{1}{\sqrt{d_i d_j}}, & \text{if } v_i \text{ and } v_j \text{ are adjacent} \\ 0, & \text{otherwise} \end{cases}$$

Let M be a symmetric matrix of order n and I be the identity matrix of order n. Then, *eigenvalues* (λ) and the *eigenvector* ($\mathbf{x}$) of M satisfy $M\mathbf{x} = \lambda\mathbf{x}$ for $\mathbf{x} \neq 0$, viz., eigenvalues are the roots of the characteristic polynomial, $\det(M - \lambda I) = 0$. The set of eigenvalues $\{\lambda_1, \lambda_2, \ldots, \lambda_n\}$ together with their multiplicities (number of occurrences of an eigenvalue λ_i) define the *spectrum* of M.

A. *Graph Energy Definitions*

Energy of a graph, $\mathcal{E}$, is captured as the sum of absolute values of its eigenvalues [14, 17]. Given a graph, its adjacency energy, $\mathcal{E}_A$, Laplacian energy, $\mathcal{E}_L$, and normalized Laplacian energy, $\mathcal{E}_{\mathcal{L}}$, differ slightly for each type of graph representation's respective eigenvalues $(\lambda(A), \lambda(L), \lambda(\mathcal{L}))$. Given an adjacency matrix of a graph, $A(G)$, the graph energy is $\mathcal{E}_A(G)$ [14]:

$$\mathcal{E}_A(G) = \sum_{i=1}^{n} |\lambda_i(A)| \tag{1}$$

The graph energy of the Laplacian matrix, $L(G)$, is $\mathcal{E}_L(G)$ [15]:

$$\mathcal{E}_L(G) = \sum_{i=1}^{n} |\lambda_i(L) - 2l/n| \tag{2}$$

in which l is the number of links and n is the number of nodes. Lastly, given the normalized Laplacian graph, $\mathcal{L}(G)$, its energy $\mathcal{E}_{\mathcal{L}}(G)$ [16] is:

$$\mathcal{E}_{\mathcal{L}}(G) = \sum_{i=1}^{n} |\lambda_i(\mathcal{L}) - 1| \tag{3}$$

Our objective in this paper is to evaluate all three types of energies when forming random graphs representing wireless networks.

B. *Energy Analysis of Regular Networks*

In an effort to understand the energy characteristics, we study several regular graphs including star, full-mesh, bus, ring, and tree with node number 10 and 100. Among these regular network structures being analyzed, we only present (due to space) three cases – star, mesh, and ring – with 10 nodes and links removal scenarios as shown in Figure 1.

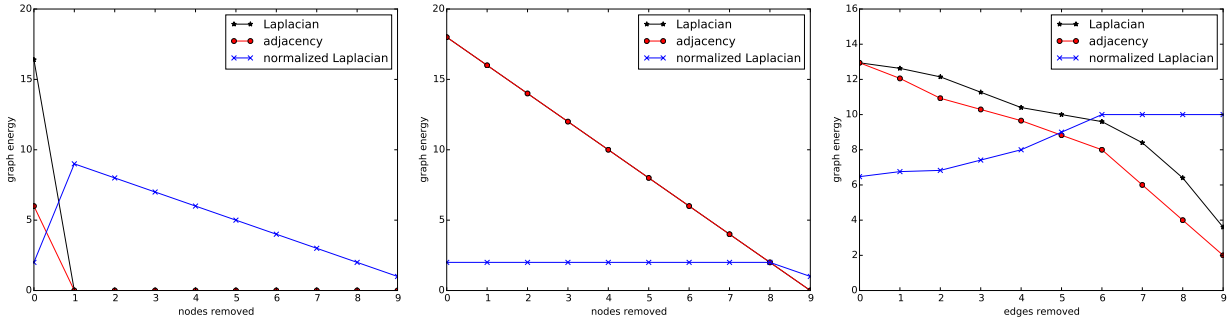

(a) Star with degree-based node removals (b) Mesh with betweenness-based node removals (c) Ring with betweenness-based edge removals

Figure 1: Energy characteristics of regular graphs (star, full-mesh, and ring) with 10 nodes

Before explaining the energies of regular graphs, we note that the eigenvalue multiplicities for adjacency, Laplacian, and normalized Laplacian matrices of star and full-mesh type graphs

are shown in Table 1. The adjacency and Laplacian eigenvalue multiplicities [18], as well as the normalized Laplacian eigenvalue multiplicities [19] vary across different graph structures.

Table 1: Eigenvalue multiplicities of star and full-mesh graph types

Matrix types		**Multiplicities**
$A(G)$	star	$\pm\sqrt{n-1}, 0^{n-2}$
	mesh	$(-1)^{n-1}, (n-1)^1$
$L(G)$	star	$0^1, 1^{n-2}, n^1$
	mesh	$0^1, n^{n-1}$
$\mathcal{L}(G)$	star	$0^1, 1^{n-2}, 2^1$
	mesh	$0^1, (\frac{n}{(n-1)})^{n-1}$

Figure 1a shows the three types of energies for a 10-node star graph (1 root node and 9 leaf nodes) as the highest degree nodes are removed iteratively. From Table 1, a star graph has its eigenvalues at $\{-\sqrt{10-1}, 0, 0, 0, 0, 0, 0, 0, 0, \sqrt{10-1}\}$. When these eigenvalues are plugged in to Equation 1, we end up with an initial adjacency energy of 6. Once the highest degree node is removed, the empty graph with isolated edges have eigenvalues of 0, thus the adjacency energy becomes 0. While a similar decreasing pattern can be observed for the Laplacian energy, the normalized Laplacian energy starts from 2, peaks to 9, and then starts a decreasing energy pattern as shown in Figure 1a. The eigenvalues of a 10-node star graph are: $\{0, 1.11, 1.11, 1.11, 1.11, 1.11, 1.11, 1.11, 1.11, 1.11\}$, and when we plug these eigenvalues to Equation 3, we end up with a starting energy of 2. Once the highest degree node is removed, the eigenvalues become 0, but due to the -1 term in Equation 3, the empty graph's energy converges to $n-1$. Adjacency and Laplacian energies behave the same in a full-mesh graph and drop at an equal rate as nodes are removed (we note that $\mathcal{E}_A(G) = \mathcal{E}_L(G)$ for regular graphs [17]), whereas the normalized Laplacian energy remains the same at 2, as shown in Figure 1b. Finally, we look into the removal of links for a ring graph (intuitively, the connectivity of a ring lies between a star and a full-mesh) as shown in Figure 1c. In the case of ring network, the starting adjacency energy (i.e. 13 from Figure 1c) lies between a star (i.e. 6 from Figure 1a) and full-mesh (i.e. 18 from Figure 1b). The normalized Laplacian energy starts around 6 and ends with an energy of 10. As the links are removed, eventually the graph becomes an empty graph with isolated nodes, each node having an eigenvalue of 0. Due to the -1 term in Equation 3, the normalized Laplacian energy converges to n for an empty graph with all isolated nodes.

III. RANDOM GRAPH MODELS

We use the following well-known graph models to generate synthetic graphs: Gilbert graph model, Erdős-Rényi graph model, and random geometric graph model. Our assumption is that these random graphs capture the probabilistic nature of wireless telemetry network connectivity. We use the Python NetworkX library to generate these synthetic graphs [20].

A. *Gilbert Graph Model (GNP)*

In the Gilbert graph model, $G(n, p)$, given n nodes, these nodes are connected via a probability of p [11]. When the $p = 0$, then the graph generated will be an empty graph (i.e. graph with no edges). When the $p = 1$, then the graph generated will be a complete graph (i.e. full-mesh graph).

B. *Erdős-Rényi Graph Model (GNL)*

The Erdős-Rényi random graph, $G(n, l)$, takes number of nodes, n, and number of links, l as input parameters and outputs a graph with random l links between pair of nodes [12]. The maximum number of links in an undirected and bidirectional graph is $\frac{n(n-1)}{2}$. For example, in this model $G(5, 10)$ will output a full-mesh graph, whereas $G(5, 8)$ will result in a graph with 5 nodes and 8 links placed between pair of nodes randomly.

C. *Random Geometric Graph Model (GEO)*

In the random geometric graph model, $G(n, r)$, n nodes are placed on a unit surface at random and then two nodes are connected if the Euclidian distance between two nodes is less then a threshold value, r [13]. For example, $G(5, 0.1)$ will place 5 nodes uniformly at random on a unit square surface. If the distance between two nodes is less than 0.1, then these two nodes will be connected. Note that in a unit square surface, maximum possible distance between any pair of nodes is $\sqrt{2}$.

IV. GRAPH ENERGY ANALYSIS OF SYNTHETIC NETWORKS

To visualize how the connectivity of wireless telemetry networks can be improved by adding links between nodes, we examine the Laplacian, adjacency, and normalized Laplacian energy across synthetic networks of varying levels of connectivity. We generate synthetic networks with 10 nodes and 100 nodes using the random graph models. For the GNP model, we vary the p value in the [0, 1] range with increments of 0.1 for both $n = 10$ and $n = 100$ cases. For the GNL model, we increment the number of links by 1 for the $n = 10$ case and 100 for the $n = 100$ case. For the GEO model, we vary the r threshold value in the [0, 2] range with increments of 0.1 for both $n = 10$ and $n = 100$ cases. We average each point in the plots 100 times and plot with the 95% confidence intervals. By using three different random graph generators, and averaging the results of our energy calculations across numerous randomly generated networks, we can make observations into the connectivity tendencies of different sized telemetry networks. The 10 node graph energy analysis of random networks is shown in Figure 2 and the 100 node graph energy analysis of random networks is shown in Figure 3.

Using a GNP random graph generator (which places connections between n nodes based on a specified probability, p), we can notice that the Laplacian and adjacency energies peak near an edge placement probability of 0.6 for both 10 node networks and 100 node networks (seen in Figure 2a and Figure 3a, respectively). After peaking, the Laplacian and adjacency energies converge at a probability of 1, where each node is connected to every other node (i.e. a full mesh network). We may notice that due to the second-order curves of the Laplacian and adjacency plot lines, that the Laplacian and adjacency energies reach the same convergence value at multiple probability

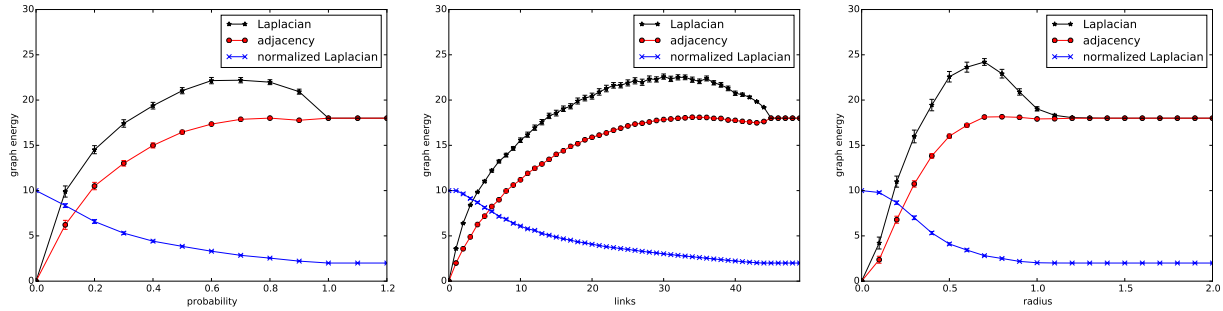

(a) 10 node GNP (b) 10 node GNL (c) 10 node GEO

Figure 2: Energy of random graphs with 10 nodes

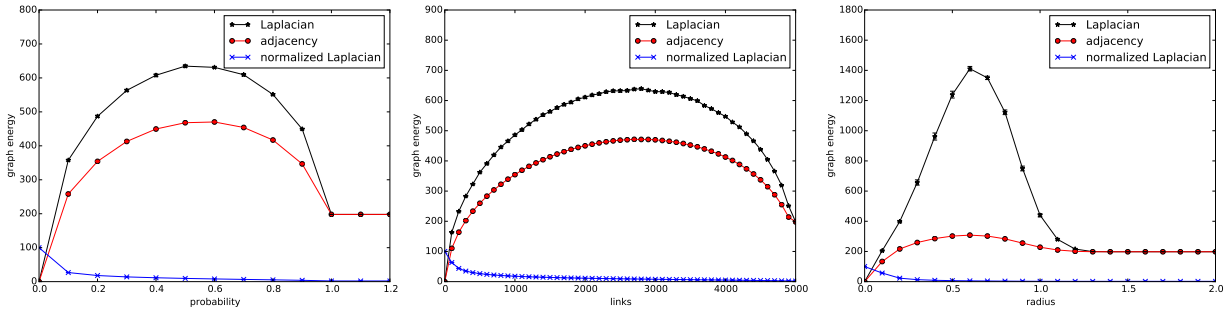

(a) 100 node GNP (b) 100 node GNL (c) 100 node GEO

Figure 3: Energy of random graphs with 100 nodes

values (e.g., 1.0 and 0.1 probability in Figure 3a). This is due to regular graphs having the same adjacency and Laplacian energy values, as explained in Section II.B. Seen most notably in the 100 node GNP plot (Figure 3a), while partially visible in the 10 node GNP plot (1.0 and 0.3 probability in Figure 2a), these matching points appear to signify varying levels of connectivity, with the lower probability point being the minimum probability for a connected graph and the larger probability (i.e., the probability when the Laplacian and adjacency energies converge) signifying full mesh connectivity. We can also observe that the normalized Laplacian energy exhibits a trend for both the 10 node networks and 100 node networks (Figure 2a and Figure 3a, respectively) where the energy gradually decreases from a peak value of n (for an n node network) at probability zero, before converging to a value at probability 1. Furthermore, we may note that the Laplacian and adjacency energies reach significantly higher peak values than the normalized Laplacian energy for both 10 node, and 100 node networks.

The GNL random graph generator produces plots similar to the GNP generator, with a notable difference being the sharpness of the Laplacian and adjacency energy peaks (seen in Figure 2b and Figure 3b); the peak value for the Laplacian and adjacency energies occurs near 30 links added for the 10 node networks, and near 3000 links added for the 100 node networks. Furthermore, we can see that the Laplacian and adjacency energies converge to a value near 18 after 45 links have been added to the 10 node networks, and converge to a value near 200 after 4950 links have been added to the 100 node networks, which are the respective points where the networks become

fully connected as full mesh networks. The normalized Laplacian energy is also very similar to the GNL generated plots (shown in Figure 2b and Figure 3b), gradually decreasing from a value of n, for a n node network, and converging after reaching full mesh connection. Moreover, we can observe that the same trend of matching points seen on the Laplacian and adjacency curves in the GNP plots (i.e., two x-axis values where the Laplacian and adjacency energies are at their convergence value) are also present in the GNL plots: the lower point being the minimum number of added links necessary for a connected graph (near 10 links added and 200 links added for 10 nodes and 100 nodes, respectively), and the upper point being when the Laplacian and adjacency energies converge at full mesh connection (near 45 links added and 5000 links added for 10 nodes and 100 nodes, respectively).

The GEO graph generator notably results in a large peak of Laplacian energy near a radius of 0.6, for both 10 node and 100 node graphs (seen in Figure 2c and Figure 3c, respectively). The adjacency energy also peaks slightly near 0.6 for both 10 node and 100 node plots, but much less prominently than the Laplacian energy peak. Additionally, at a radius of approximately 1.4, we see that the Laplacian and adjacency energies appear to converge to the same value. Similar to the GNP and GNL plots, matching points can be observed where the Laplacian and adjacency energies reach their convergence value: the lower point (radius near 0.4 and 0.2 for 10 node and 100 node graphs, respectively) being the minimum radius for a connected graph, and the upper point (radius near 1.4 for both 10 node and 100 node graphs) being the radius at which the Laplacian and adjacency energies converge and reach full mesh connection. Furthermore, we can observe that the normalized Laplacian energy behaves similarly across all three graph generators, decreasing from n (for an n-node network) to its convergence value, which occurs near radius 1.4 for the GEO generator plots.

V. CONCLUSIONS

Network science tools enable analysis of the structure and predict the behavior of dynamic wireless networks. In this paper, we modeled the wireless telemetry network scenario using three random graph models: Gilbert, Erdős-Rényi, and random geometric graph models. We analyze the structure of these randomly generated graphs using the graph energy metric, which captures the sum of absolute values of eigenvalues. The synthetically generated Gilbert and Erdős-Rényi random graphs resulted in similar graph energy measurements. Among the graph energy measurements we conduct, adjacency and Laplacian energy measurements are second-order curves as the graphs converge to being complete graphs. The normalized Laplacian energy consistently decreases and approaching to the theoretical lower bound.

In our future work, we will investigate the reasoning of the second-order curves for adjacency and Laplacian energy relating to the connectivity of the graphs. We also plan to use realistic mobility models to model and study mobile wireless networks.

Acknowledgment

We would like to acknowledge members of the Complex Networks and Systems (CoNetS) group for discussions on this work. Tristan A. Shatto is in part supported by Missouri University

of Science and Technology (Missouri S&T) Opportunities for Undergraduate Research Experiences (OURE) Program. This work was also funded in part by the International Foundation for Telemetering (IFT).

REFERENCES

[1] National Research Council, *Strategy for an Army Center for Network Science, Technology, and Experimentation*. Washington, DC: The National Academies Press, 2007.

[2] L. Gharai, K. Guan, and R. Ghanadan, "Military Scenarios and Solutions from a Network Science Perspective," in *Proceedings of the IEEE Military Communications Conference (MILCOM)*, pp. 1–6, October 2009.

[3] P. M. Dudas, "Cooperative, Dynamic Twitter Parsing and Visualization for Dark Network Analysis," in *Proceedings of the IEEE 2nd Network Science Workshop (NSW)*, (West Point, NY), pp. 172–176, April 2013.

[4] C. Arney, K. Coronges, H. Fletcher, J. Hagen, K. Hutchinson, A. Moss, and C. Thomas, "Using Rare Event Modeling & Networking to Build Scenarios and Forecast the Future," in *Proceedings of the IEEE 2nd Network Science Workshop (NSW)*, (West Point, NY), pp. 31–36, April 2013.

[5] P. Holme and J. Saramäki, "Temporal networks," *Physics Reports*, vol. 519, pp. 97–125, October 2012.

[6] J. P. Rohrer, A. Jabbar, E. K. Çetinkaya, and J. P. Sterbenz, "Airborne telemetry networks: Challenges and solutions in the ANTP suite," in *Proceedings of the IEEE Military Communications Conference (MILCOM)*, (San Jose, CA), pp. 74–79, November 2010.

[7] L. d. F. Costa, F. A. Rodrigues, G. Travieso, and P. R. Villas Boas, "Characterization of complex networks: A survey of measurements," *Advances in Physics*, vol. 56, no. 1, pp. 167–242, 2007.

[8] T. A. Shatto and E. K. Çetinkaya, "Spectral Analysis of Backbone Networks Against Targeted Attacks," in *Proceedings of the 13th IEEE/IFIP International Conference on the Design of Reliable Communication Networks (DRCN)*, (Munich), March 2017.

[9] T. A. Shatto and E. K. Çetinkaya, "Variations in Graph Energy: A Measure for Network Resilience," in *9th IEEE/IFIP International Workshop on Reliable Networks Design and Modeling (RNDM)*, (Sardinia), May 2017. Submitted.

[10] E. K. Çetinkaya and T. A. Shatto, "Eigenvalues for Resilience Analysis of Backbone Networks," in *Proceedings of the SIAM Workshop on Network Science (NS)*, (Pittsburgh, PA), July 2017.

[11] E. N. Gilbert, "Random Graphs," *The Annals of Mathematical Statistics*, vol. 30, no. 4, pp. 1141–1144, 1959.

[12] P. Erdős and A. Rényi, "On random graphs I.," *Publicationes Mathematicae Debrecen*, vol. 6, pp. 290–297, 1959.

[13] M. Penrose, *Random Geometric Graphs*. Oxford Studies in Probability 5, 2003.

[14] I. Gutman, "The Energy of a Graph: Old and New Results," in *Proceedings of the Euroconference Algebraic Combinatorics and Applications (ALCOMA)*, (Gößweinstein, Germany), pp. 196–211, September 1999.

[15] I. Gutman and B. Zhou, "Laplacian energy of a graph," *Linear Algebra and its Applications*, vol. 414, no. 1, pp. 29–37, 2006.

[16] M. Cavers, S. Fallat, and S. Kirkland, "On the normalized Laplacian energy and general Randić index R_{-1} of graphs," *Linear Algebra and its Applications*, vol. 433, no. 1, pp. 172–190, 2010.

[17] X. Li, Y. Shi, and I. Gutman, *Graph Energy*. Springer New York, 2012.

[18] A. E. Brouwer and W. H. Haemers, *Spectra of Graphs*. Springer New York, 2012.

[19] F. R. K. Chung, *Spectral Graph Theory*. American Mathematical Society, 1997.

[20] A. A. Hagberg, D. A. Schult, and P. J. Swart, "Exploring Network Structure, Dynamics, and Function using NetworkX," in *Proceedings of the 7th Python in Science Conference (SciPy)*, (Pasadena, CA), pp. 11–15, August 2008.